Journal of Microwaves, Optoelectronics and Electromagnetic Applications, Vol. 20, No. 2, June 2021
DOI: http://dx.doi.org/10.1590/2179-10742021v20i21157

Compact Triple Band Notched Pentagonal Shaped UWB Antenna Loaded with Slots and Parasitic Resonator

Ameya A. Kadam[1], Amit A. Deshmukh[2]
[1]*Research Scholar, EXTC Department, SVKM's DJSCE, Mumbai, India, ameyakadam@rediffmail.com*
[2]*Professor & Head, EXTC Department, SVKM's DJSCE, Mumbai, India,amitdeshmukh76@rediffmail.com*

***Abstract*— In this paper, a compact, planar printed microstrip line fed pentagonal shape ultra-wideband antenna with triple band-notched characteristics is proposed and investigated. By incorporating a pair of mirrored Γ-shape, a pair of mirrored L-shape slots in the pentagonal patch and bent C-shape parasitic strip at the backside of a patch, the tunable band notched responses are realized. The proposed antenna is fabricated on Rogers RO3003 substrate with permittivity 3.0 and thickness of 0.76 mm. The measured results indicate that the proposed antenna having dimensions of 32 × 24 × 0.76 mm^3 has a bandwidth over the frequency band 2.7-10.6 GHz with $S_{11} \leq -10$ dB (VSWR ≤ 2), except in WiMAX band (3.27-3.85 GHz), WLAN band (5.6-5.95 GHz) and ITU-T band (7.84-8.46 GHz). The presented antennas show dipole-like patterns in E-plane and omnidirectional in H-plane, minor group delay variation, and nearly constant gain at operating frequencies.**

***Index Terms*—** L-shape slot, Parasitic resonator, Triple band-notch characteristics, Ultra-wideband pentagonal patch

I. INTRODUCTION

Ultra-wideband (UWB) wireless communication technology has been receiving wide impetus since the Federal Communication Commission unlicensed the frequency band of 3.1-10.6 GHz for communication purposes [1]. The frequently used forms of radiating patch in UWB planar antennas are square, circular [2]; crescent-shape [3]; sectoral [4]; elliptical [5]; and their amended variations as they can be easily incorporated with microwave integrated circuits, lightweight and low profile in nature. In the designated UWB spectrum other services such as WiMAX, WLAN, IEEE 802.16 (3.3–3.7 GHz), IEEE 802.11a, ITU-T (8.02– 8.4 GHz band) exist. Hence, it is necessary to develop a UWB antenna with notched frequency responses to reduce the probable interferences between mentioned narrowband and UWB systems.

Numerous designs of antenna have been reported for notched frequency responses in ultra-wideband. The reported designs include incorporating an elliptical slot within circular monopole [6]; two annular ring-shape slots with half-wavelength dimensions at a notched frequency in the radiating patch [7]; attaching open-circuited stubs at the ends of plus-shape patch [8]; attaching quarter wavelength stubs to quasi U-shape patch [9]. By incorporating a split ring resonator (SRR) in the feedline, band rejection of WLAN has been achieved [10]. A slotline resonator within the feedline of

Brazilian Microwave and Optoelectronics Society-SBMO *received 13 Dec 2020; for review 28 Dec 2020; accepted 8 Apr 2021*
Brazilian Society of Electromagnetism-SBMag *© 2021 SBMO/SBMag* CC BY *ISSN 2179-1074*

the antenna has been incorporated to reject the band assigned for the HIPERLAN/2 and IEEE802.11a [11]. Other techniques to achieve band notch response involves incorporating slots in the ground plane such as a pair of symmetrical L-shape slots [12]; C-shape slots [13]. Also, new antenna designs a combination of techniques to realize notch responses have been implemented. Triple notched band elimination of WLAN, WiMAX, and Downlink Satellite System bands is realized due to etching of slots and insertion of stub [14]. The square-shape electromagnetic band gap (EBG) with defected ground plane designs is used to realize band notch function in WiMAX and WLAN bands [15]. By incorporating two EBG structures, notch band responses for WiMAX and WLAN bands are obtained [16]. As per available literature, the addition of stubs, incorporation of slots in radiating patch or ground plane provides impedance mismatch, which consequences in notch response. However, while selecting the slot or stub location, a thorough explanation for the modal currents on the patch or ground plane, at respective resonant modes, is not given.

In this paper, first for microstrip line fed regular pentagonal microstrip antenna (PMSA), effects of variation in backed offset ground plane on patch modal frequencies are studied. As the length of a ground plane decreases, the overlapping substrate area between patch and ground plane decreases. This reduces the effective dielectric constant of the cavity. This change in effective dielectric constant alters the fundamental and higher-order mode frequencies of the patch. Using this study, it is clearly shown that fundamental and higher-order modes in printed monopole patch are the modified half-wavelength modes and their variations as against quarter wavelength mode variations. Further, a novel design of UWB antenna with pentagonal shape incorporated with a pair of mirrored Γ-shape and L-shape slots in the patch along with bent C-shape parasitic resonator on the backside of a patch for triple band notch responses is proposed. Initially, the microstrip line fed pentagonal shape UWB antenna is designed. For frequencies, 2.94 - 11 GHz, the impedance bandwidth for $S_{11} \leq$ -10 dB is obtained for the UWB antenna. Later, using optimized pentagonal shape UWB antenna with mirrored Γ- and L-shape slots along with bent C-shape parasitic resonator, a notch response over three frequency bands at 3.35 - 3.81 GHz (WiMAX), 5.6 - 5.97 GHz (WLAN), and 7.94 - 8.48 GHz (ITU-T) is realized. The tunable band notch characteristics can be attained in WiMAX, WLAN, and ITU-T band by changing dimensions of Γ-shape slots, L-shape slots, and a parasitic strip respectively. The proposed structures were optimized on Rogers RO3003 substrate using Computer Simulation CST2019), followed by the frequency and time-domain measurements. Using Keysight Technologies make VNA (N9917A) the reflection coefficient (S_{11}) and time-domain characteristics of the antenna are measured whereas far-field radiation patterns and peak gain are measured using Rohde and Schwarz make signal generator (SMB 100A) and spectrum analyzer (FSC-6). The tunable band notch benefits in the reduction of interference with simultaneous applications such as WiMAX, WLAN. The novelty of the paper is the inclusion of modal analysis about a mismatch of impedance to realize the notch responses along with compactness of the structure.

Brazilian Microwave and Optoelectronics Society-SBMO *received 13 Dec 2020; for review 28 Dec 2020; accepted 8 Apr 2021*
Brazilian Society of Electromagnetism-SBMag *© 2021 SBMO/SBMag* CC BY *ISSN 2179-1074*

II. PMSA BACKED BY GROUND PLANE

The PMSA of dimensions, side length s = 12.5 mm with ground plane of size L_g = 32mm and W_g = 24mm, on Rogers RO3003 substrate (ε_r = 3, h = 0.76 mm, $tan\ \delta$ = 0.0019) is shown in *Fig.* 1(a, b). A feed microstrip line having a width of 2mm for 50 Ω impedance, has been selected to excite the pentagonal patch. The resonance curve plot for PMSA for L_g = 32 mm, shows excitation of TM_{11} and TM_{21} modes as shown in *Fig.* 1(c). In the pentagonal shape antenna, the first two resonant modes are referred to as TM_{11} and TM_{21}, as they resemble the mode distributions present in the circular patch, having the same patch area. As the length of the ground plane, L_g goes on reducing keeping other parameters constant, TM_{11} and TM_{21} modal frequencies increase. The resonance curve plots for the same exhibiting variations in modal frequencies are given in *Fig.* 1(c). This frequency increment is attributed to a decrease in effective dielectric constant (ε_{re}) due to a reduction in dimension of the backing ground plane. The impedance at TM_{11} modal frequency decreases since the quality factor of structure goes on decreasing.

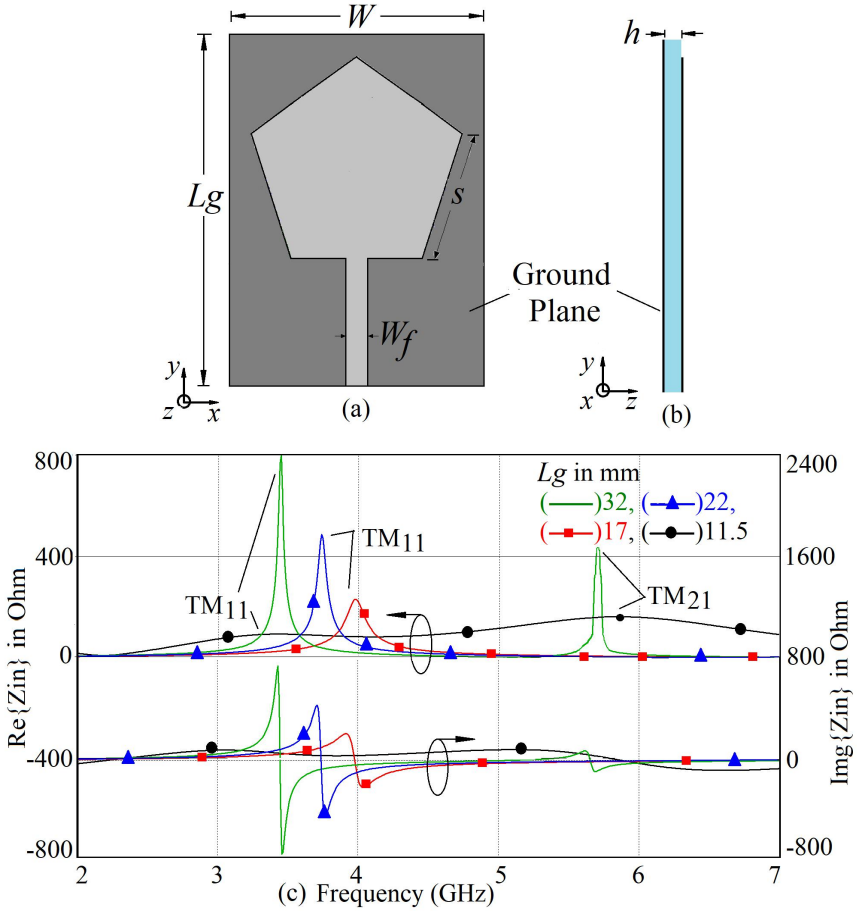

Fig. 1. PMSA backed by square ground plane (a) Front View, (b) Side View and its (c) resonance curve plots for variation in length of ground plane *Lg*.

Further, when L_g = 11.5 mm the ground plane exactly below the patch gets vanished resulting in a decrement in TM_{11} mode frequency. This decrement in frequency is due to an increase in fringing field length due to the absence of the ground plane exactly below the pentagonal patch. Thus, it can be inferred from resonance curves and surface current distributions that, fundamental and next higher-

received 13 Dec 2020; for review 28 Dec 2020; accepted 8 Apr 2021
© 2021 SBMO/SBMag
ISSN 2179-1074

order modes in printed pentagonal monopole patch are similar to modes of PMSA and they show multiples of half-wavelength variations [26]. The absence of the ground plane exactly below the patch results in a lower quality factor which leads to wider bandwidth at the resonances for fundamental and higher-order modes. The average and vector surface current distributions at TM_{11} and TM_{21} mode for different values of ground plane length L_g are shown in *Fig*. 2(a-h).

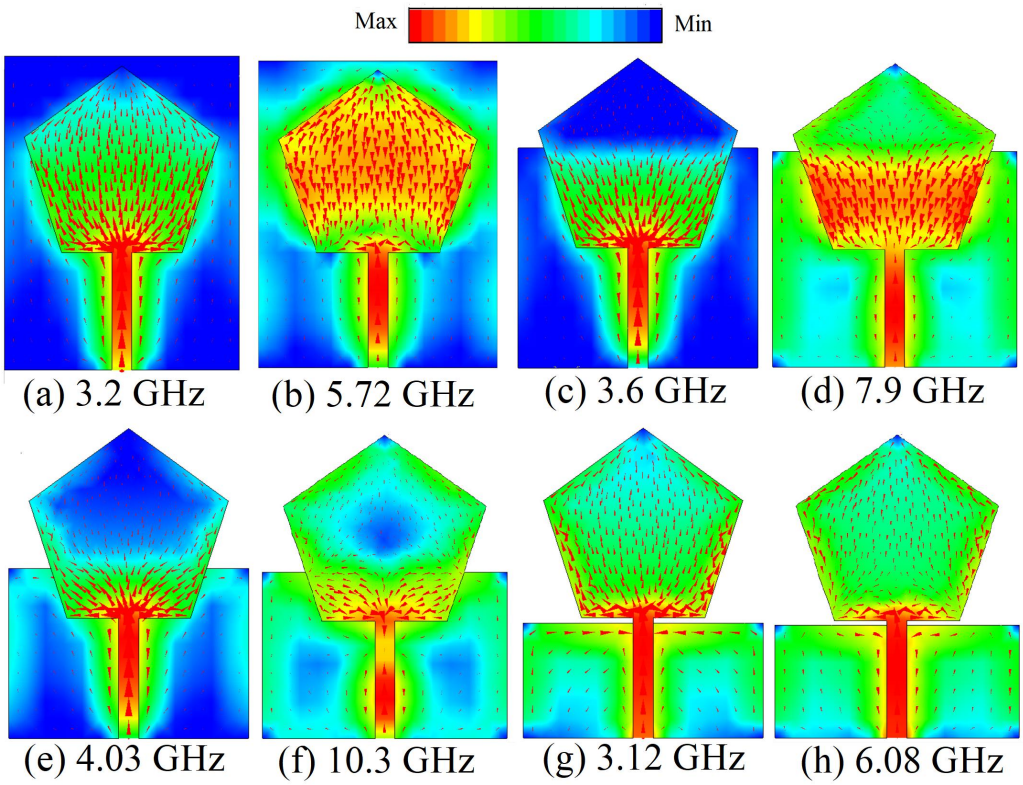

Fig. 2. Surface current distribution at TM_{11} and TM_{21} modes for different length of ground plane L_g in mm (a,b) 32, (c, d) 22, (e, f) 17, and (g, h) 11.5.

III. PENTAGONAL UWB PATCH ANTENNA

The pentagonal shape UWB antenna is designed on Rogers RO30003 substrate which has thickness h = 0.76 mm, dielectric constant ε_r = 3.0, and loss tangent $tan\ \delta$ = 0.001. The pentagonal patch having side length s = 12.5 mm is selected so that fundamental TM_{11} mode frequency is near 3.12 GHz while lower band edge frequency is around 2.97 GHz. A microstrip line having a width of 2 mm with a ground plane having dimensions L_g = 11.5 mm and W_g = 24 mm, has been used to feed the signal to the antenna. The horizontal separation between patch and ground plane (p) is taken equal to 0.5 mm, which yields optimum bandwidth. For the frequencies 2-11 GHz, the resonance curve, simulated and measured input impedance plots are shown in *Fig.* 3(a). The impedance bandwidth for the antenna with $S_{11} \leq$ -10dB has been obtained in the frequency range 2.9 GHz to greater than 10.6 GHz. The fabricated prototype of the UWB antenna is shown in *Fig.* 3(b, c). In printed monopole antenna using a pentagonal patch, resonant modes are TM_{11}, TM_{21}, and TM_{02} as they are analogous to that of circular shape printed monopole having the same area. The simulated surface current distribution of the UWB antenna for TM_{11}, TM_{21}, and TM_{02} modes is shown in *Fig.* 3(d-f).

received 13 Dec 2020; for review 28 Dec 2020; accepted 8 Apr 2021
© 2021 SBMO/SBMag
ISSN 2179-1074

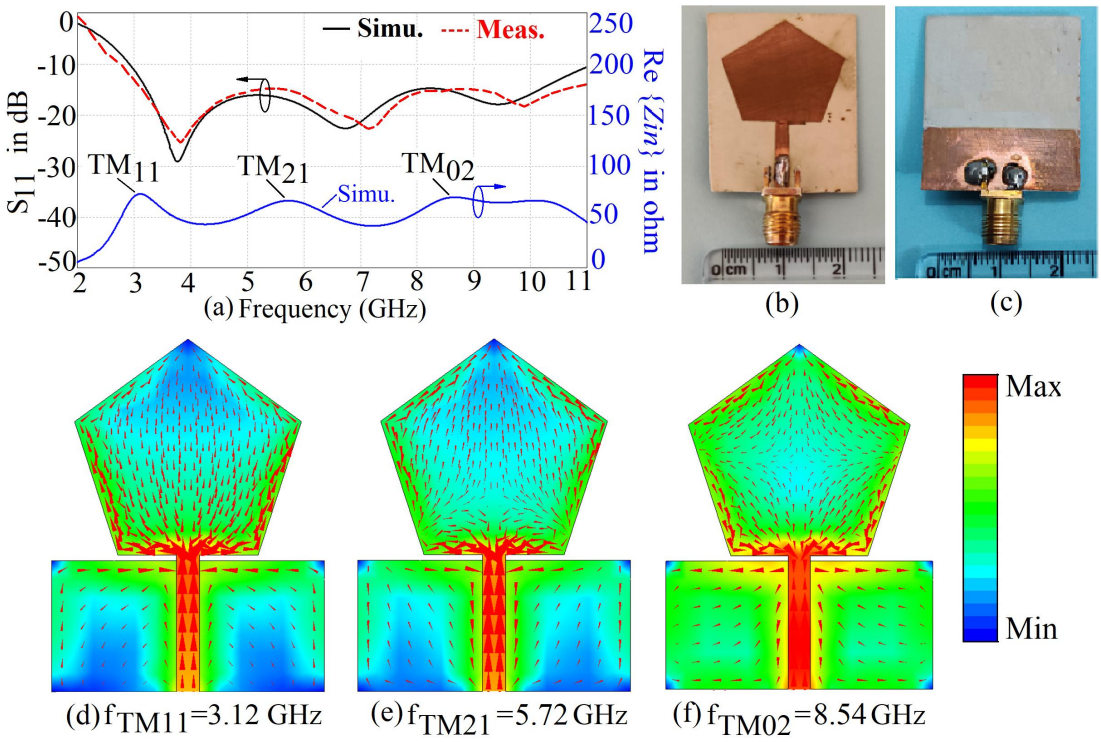

Fig. 3. (a) Simulated resonance curve and S_{11} plots, (b, c) fabricated prototype of UWB antenna, and simulated surface current distribution at (d) f_{TM11} = 3.12 GHz, (e) f_{TM21} = 5.72 GHz and (f) f_{TM02}= 8.54 GHz for pentagonal UWB patch antenna.

IV. PENTAGONAL SHAPE TRIPLE BAND NOTCHED UWB ANTENNA

Further, in this paper novel design of pentagonal shape UWB antenna for triple notch responses in WiMAX, WLAN and ITU-T band is presented with two mirrored Γ-shape and L-shape slots and bent C-shape parasitic resonator. The evolution of antenna structure to realize triple band notched responses is shown in *Fig.* 4(a-d). The optimised dimensions of the proposed antenna are L = 32, W = 24, L_g = 11.5, W_f = 2, h = 0.76, s = 12.5, p = 0.5, L_{h1} = 5, L_{v1} = 11, L_{h2} = 3, L_{v2} = 10, L_{h3} = 21, L_{v3} = 6, y_1 = 26, y_2 = 12.5, y_3 = 16, W_s = 0.5. All dimensions are in mm. The effect of incorporating slots and parasitic resonator is investigated subsequently in detail by analysing the resonance plot of the antenna.

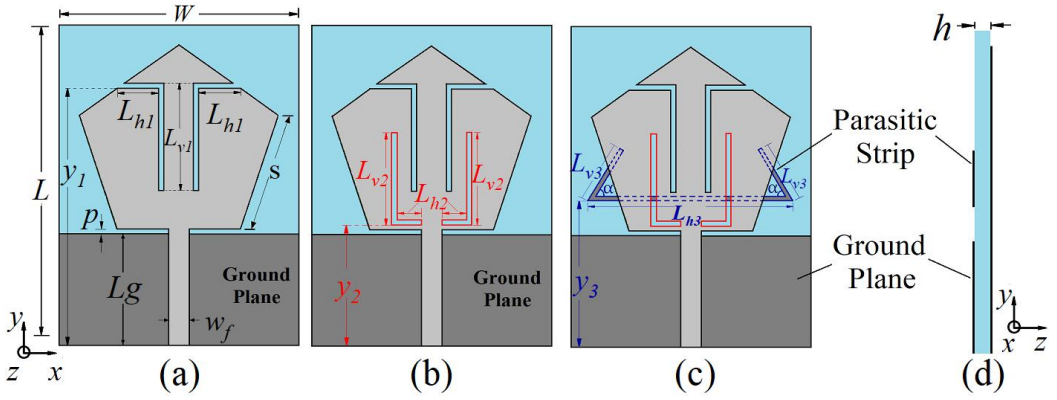

Fig. 4. The design evolution of the triple band notch antenna (a) pair of Γ -shape slots, (b) pair of L-shape slots, (c) bent C-shape parasitic resonator loaded Pentagonal patch antenna and its (d) side view antenna.

© 2021 SBMO/SBMag CC BY
ISSN 2179-1074

A. Effect of the Γ-shape slots

The effect of mirrored Γ-shape slot on antenna structure is investigated in terms of modal frequency distribution and corresponding input impedance (Z_{in}). Initially, the only horizontal slot with length L_{h1} is incorporated. The position of this slot is selected so that it effectively perturbs the current distribution in the patch present at TM_{21} mode. As L_{h1} is increased, the input impedance corresponding to TM_{21} mode also increases as shown in *Fig.* 5(a). Further, to increase the impedance at this TM_{21} mode significantly the vertical slots with dimension L_{v1} have been incorporated which results in the formation of two mirrored Γ-shape slots as shown in *Fig.* 5(b). As L_{v1} increases the impedance of TM_{21} mode initially increases beyond 150 Ω and then decreases such that Z_{in} between TM_{11} and TM_{21} modes goes below 25 Ω resulting in notch characteristics as shown in *Fig.* 5(b). However, the TM_{11} resonant mode frequency of the patch remains unaltered. As seen from *Fig.* 5(b), the dimension of slot L_{h1} = 5 mm and L_{v1} = 11 mm results in simulated S_{11} greater than -10 dB (VSWR ≥ 2) in the frequency spectrum 3.35 - 3.81 GHz resulting in notch response in WiMAX band.

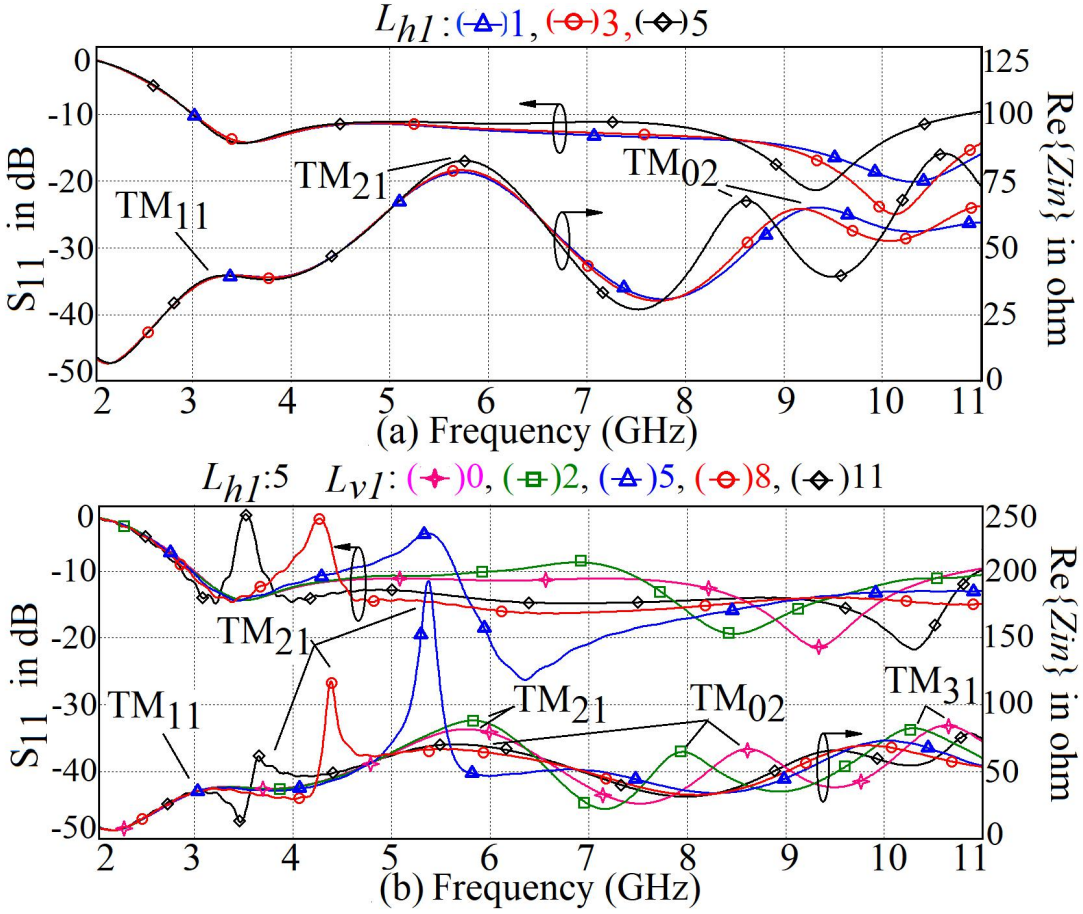

Fig. 5. Simulated resonance curve plots and magnitude of S_{11} for variation in (a) L_{h1} and (b) L_{v1} for Γ-shape slot loaded pentagonal UBW antenna (dimensions in mm).

B. Effect of the L-shape slots

The effect of pair of mirrored L-shape slots incorporated in antenna structure is investigated in terms of modal frequency distribution and corresponding impedance. Initially, a pair of vertical slots with dimension L_{v2} in the pentagonal patch is incorporated. The positions of these vertical slots are

© 2021 SBMO/SBMag CC BY
ISSN 2179-1074

selected such that it effectively perturbs current distribution in the patch present at TM_{31} mode resulting in notch response. As L_{v2} is increased, the resonance frequency corresponding to TM_{31} mode gets lowered, but Z_{in} at this mode gets increased beyond 75 Ω. As seen from *Fig.* 6(a), for L_{v2} = 10 mm, the notch response is obtained in the frequency band 9.48 to 9.89 GHz, however, TM_{11}, TM_{21}, and TM_{02} resonant mode frequencies of patch remains unaltered. To further perturb the current distribution at TM_{31} mode, the horizontal slots with dimension L_{h2} are incorporated near the feedline resulting in the formation of mirrored L-shape slots. *Fig.* 6(b) shows the effect of variation of L_{h2} for the constant value of L_{v2} = 10 mm on S_{11} and the resonance curve. As L_{h2} is increased from 1.5 to 3 mm, the input impedance at TM_{31} mode gets increased from 75 Ω to more than 200 Ω. This significant impedance mismatch results in notch characteristics with high rejection capability. As seen from *Fig.* 6(b), the dimensions of the slot L_{h2} = 3 mm and L_{v2} = 10 mm results in simulated S_{11} greater than -10 dB (VSWR ≥ 2) in the frequency band 7.9 - 8.42 GHz resulting in notch response in ITU-T band.

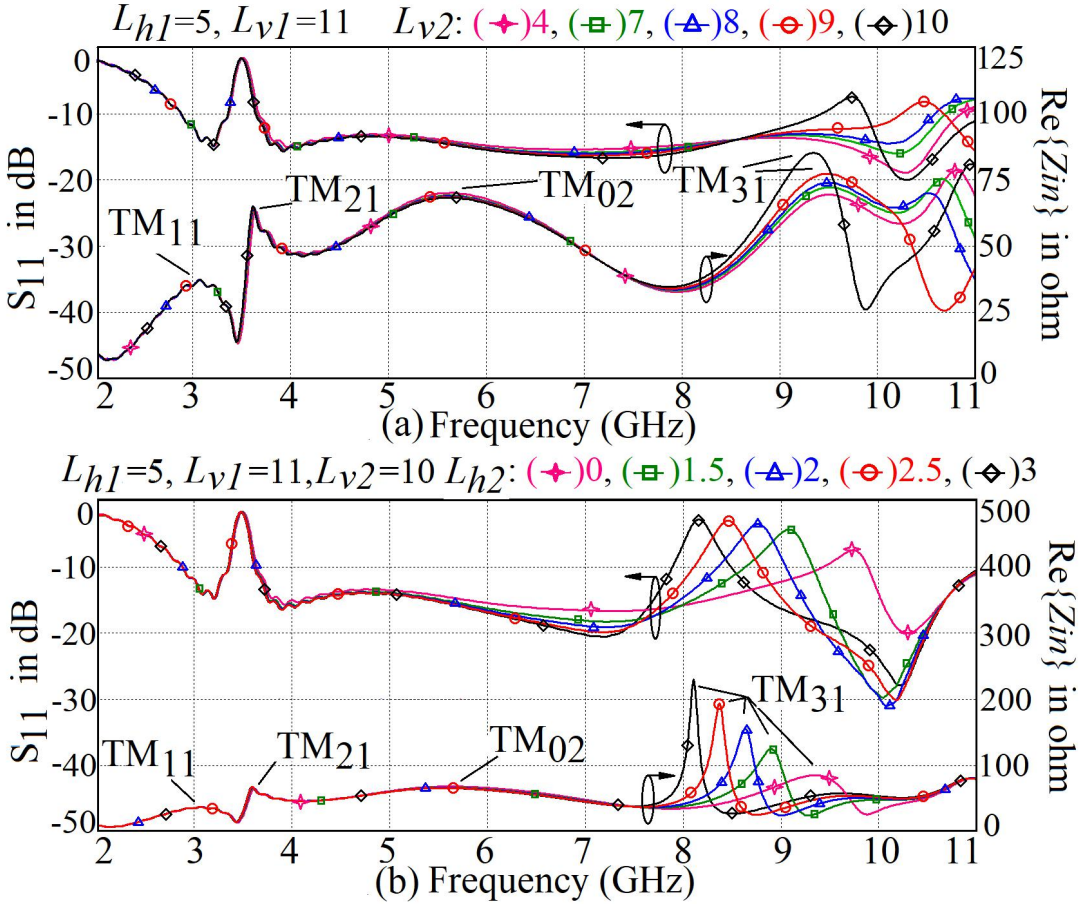

Fig. 6. Simulated resonance curve plots and magnitude of S_{11} for variation in (a) L_{v2} and (b) L_{h2} for L-shape slot loaded pentagonal UBW antenna. (dimensions in mm).

C. Effect of addition of bent C-shape parasitic strip

Further, the effect of the addition of bent C-shape parasitic strip on S_{11} and input impedance is investigated. Bent C-shape parasitic strip designed on the backside of the patch has horizontal length L_{h3}, each inclined strip length L_{v3} subtending angle α placed symmetrically about the microstrip feed

© 2021 SBMO/SBMag CC BY
ISSN 2179-1074

line to realize good band-notched characteristic in WLAN band which increases the input impedance at TM_{02} mode. *Fig.* 7(a, b) shows the plot of simulated S_{11} against frequency for different values of vertical strip dimension L_{v3} and horizontal strip dimension L_{h3}. As the length of horizontal strip, L_{h3} is increased from 9 to 21 mm keeping $\alpha = 60^{o}$ and $L_{v3} = 6$ mm, the centre frequency of the notched band is shifted from 7.1 GHz to 5.72 GHz as shown in *Fig.* 7(a). Later, as the length of vertical strip L_{v3}, is increased from 2 to 6 mm keeping $\alpha = 60^{o}$ and $L_{h3} = 21$ mm, the notched band centre is shifted from 6.98 GHz to 5.72 GHz as shown in *Fig.* 7(b). The reduction in notched band centre frequency is attributed to an increase in the resonating length of the parasitic resonator. For $L_{h3} = 21$ mm, the input impedance of TM_{02} goes above 275 Ω resulting in a notch response in the frequency band 5.6-6.03 GHz.

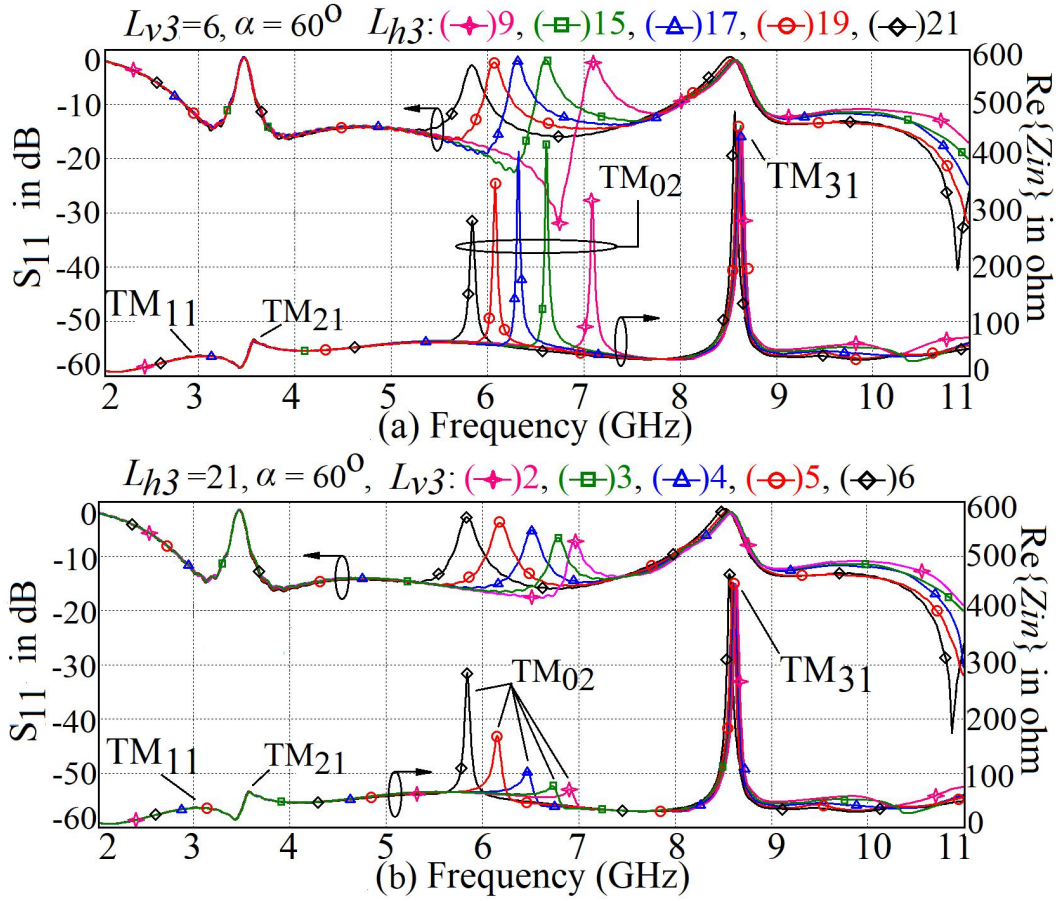

Fig. 7. Simulated resonance curve plots and S_{11} for (a) varying vertical dimension L_{v3}, and (b) varying horizontal dimension of parasitic resonator L_{h3} (dimensions in mm).

The length of the parasitic resonator L_{pr} for the chosen notched frequency on the substrate with dielectric constant ϵ_r and thickness h is approximately found using the following expressions [27]:

$$L_{pr} = \frac{\lambda_g}{2} = \frac{\lambda_0}{2\sqrt{\varepsilon_{eff}}} = \frac{c}{2 * f_{notch} * \sqrt{\varepsilon_{eff}}} \tag{1}$$

$$\varepsilon_{eff} = \frac{\varepsilon_r + 1}{2} + \frac{\varepsilon_r - 1}{2}\left(1 + \frac{12h}{w_s}\right)^{-1/2} \tag{2}$$

received 13 Dec 2020; for review 28 Dec 2020; accepted 8 Apr 2021
© 2021 SBMO/SBMag CC BY
ISSN 2179-1074

Here, λ_g is the guided wavelength, $\lambda_0 = c/f_{notch}$ is the free space wavelength, c is the velocity of light, f_{notch} is the frequency of the notched band centre, ϵ_{eff} is the effective dielectric constant, and w_s is the width of the strip. For the optimized dimension using equation (2), the effective permittivity ϵ_{eff} is calculated as 2.23. Using equations (1) and (2), it is verified that, half of the length of bent C-shape parasitic resonator is $(L_{h3}/2) + L_{v3}$ = 16.5 mm, which is nearly equal to $\lambda_g/2$ obtained at the centre frequency 5.75 GHz which is 16.81 mm.

D. Results and Discussions

Based on the above parametric study, a pentagonal-shape triple band notch antenna is fabricated on 0.76 mm thick Rogers RO3003 substrate. The microstrip line feed at one end is connected to a panel type SMA connector having 50-Ω characteristic impedance. The plots of the simulated and measured S_{11} are shown in *Fig.* 8(a) indicates that the antenna has an impedance bandwidth over the frequency band 2.72 - 10.6 GHz with $S_{11} \leq$ -10 dB, excluding at 3.35 - 3.81 GHz, 5.6 - 5.97 GHz, and 7.94 - 8.48 GHz. The misalignment of the location of notches and depths in simulated and measured results are due to the tolerances in circuit fabrication that can be probably attributed to fabrication faults, defectiveness in the substrate permittivity, non-consideration of SMA connector in simulation. The simulated average and vector current distribution at notched frequencies of these bands is shown in *Fig.* 8(b-d).

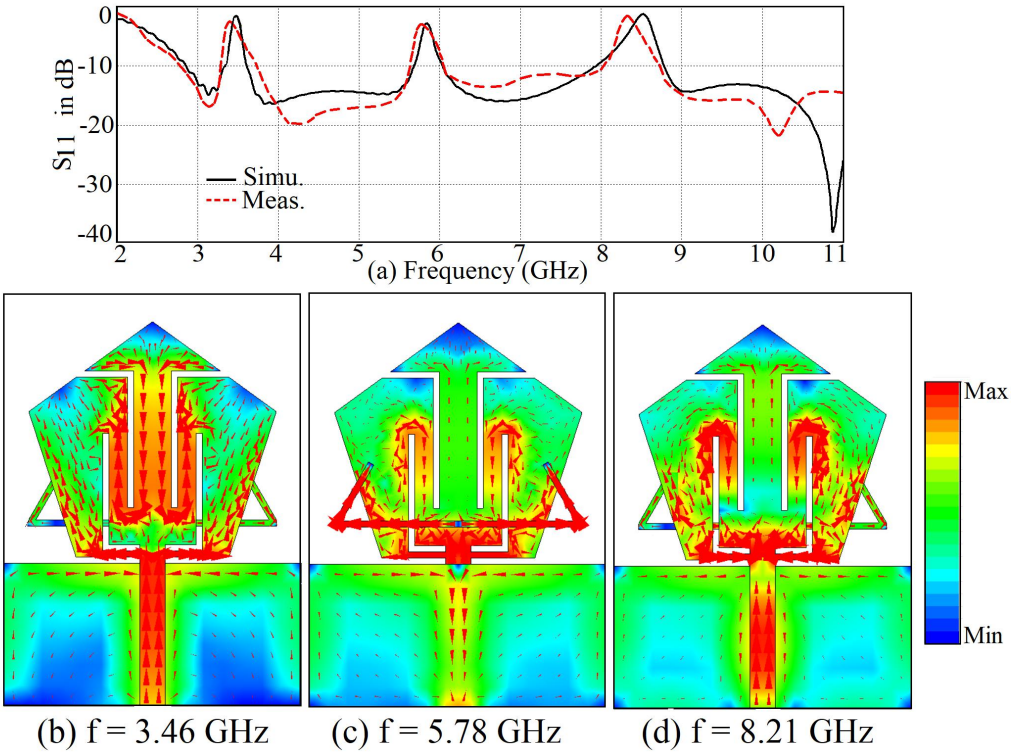

Fig. 8. (a) Measured and simulated S_{11} for proposed triple band notch antenna, its simulated surface current distribution at the notched frequencies, (b) 3.46 GHz, (c) 5.78 GHz and (d) 8.21 GHz.

As seen from *Fig.* 8(b, d), the current is mainly concentrated around a pair of mirrored Γ- and L-shape slots. At notched frequencies, the currents are in opposite directions around the slots canceling

received 13 Dec 2020; for review 28 Dec 2020; accepted 8 Apr 2021
© 2021 SBMO/SBMag
ISSN 2179-1074

the radiation. With a bent C-shape parasitic resonator on the backside of the patch, the currents are strongly concentrated in the resonator and are opposite in direction to that in the patch at notched frequencies as seen from *Fig.* 8(c). The front and back views of the fabricated prototype of triple band notched pentagonal shape antenna are shown in *Fig.* 9(a) and (b) respectively.

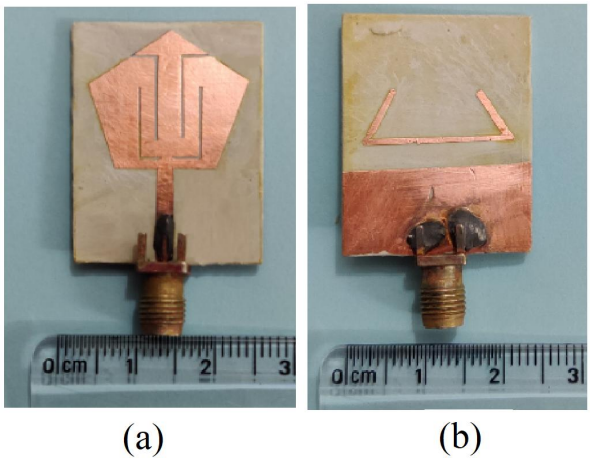

Fig. 9. The fabricated prototype of a triple band notch antenna (a) Front and (b) Back views.

The far-field pattern and gain of these antennas were measured using Rohde & Schwarz make SMB 100A signal generator and FSC-6 spectrum analyser with more than $2D^2/\lambda_0$ distance between standard horn antennas of the corresponding frequencies and proposed antenna, where D is taken as maximum dimension of antenna ensuring minimum reflection surroundings. The simulated and measured gain plots of UWB antenna and triple band-notched antenna till 8 GHz are shown in *Fig.* 10. The gain of the antenna is between 2 to 4 dB over the 3.0 - 8.0 GHz frequency range excluding notched frequency bands which ensures that band-notched responses are good. The normalized measured radiation patterns at 4.2, 5.4, and 7.2 GHz in the principal planes are shown in *Fig.* 11. The antenna exhibits an almost omnidirectional far-field pattern in the H-plane and a figure of eight patterns in the E-plane at these frequencies. Slight variations noted between simulated and measured results are happened to be because of cable losses, reflected waves from surroundings, fabrication error.

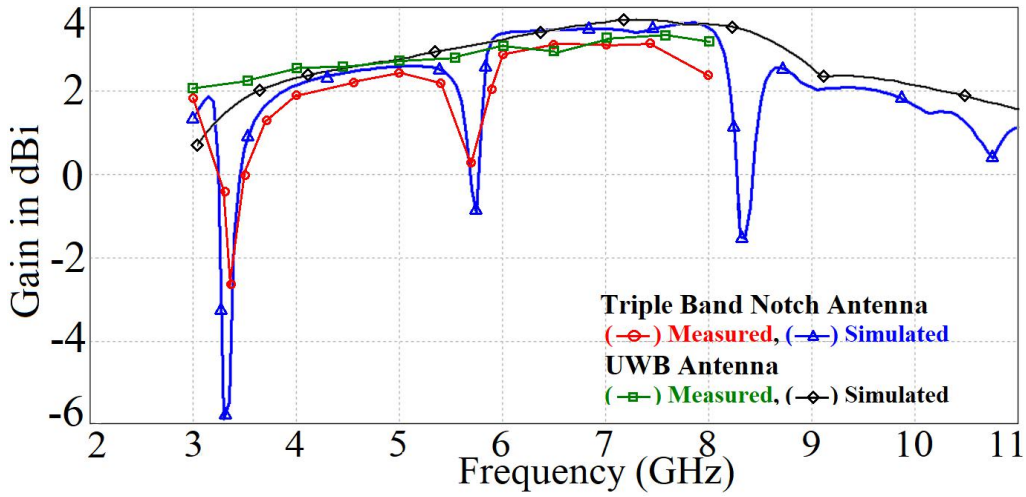

Fig. 10. Gain plot for the pentagonal shape UWB antenna and triple-band notch antenna.

received 13 Dec 2020; for review 28 Dec 2020; accepted 8 Apr 2021
© 2021 SBMO/SBMag
ISSN 2179-1074

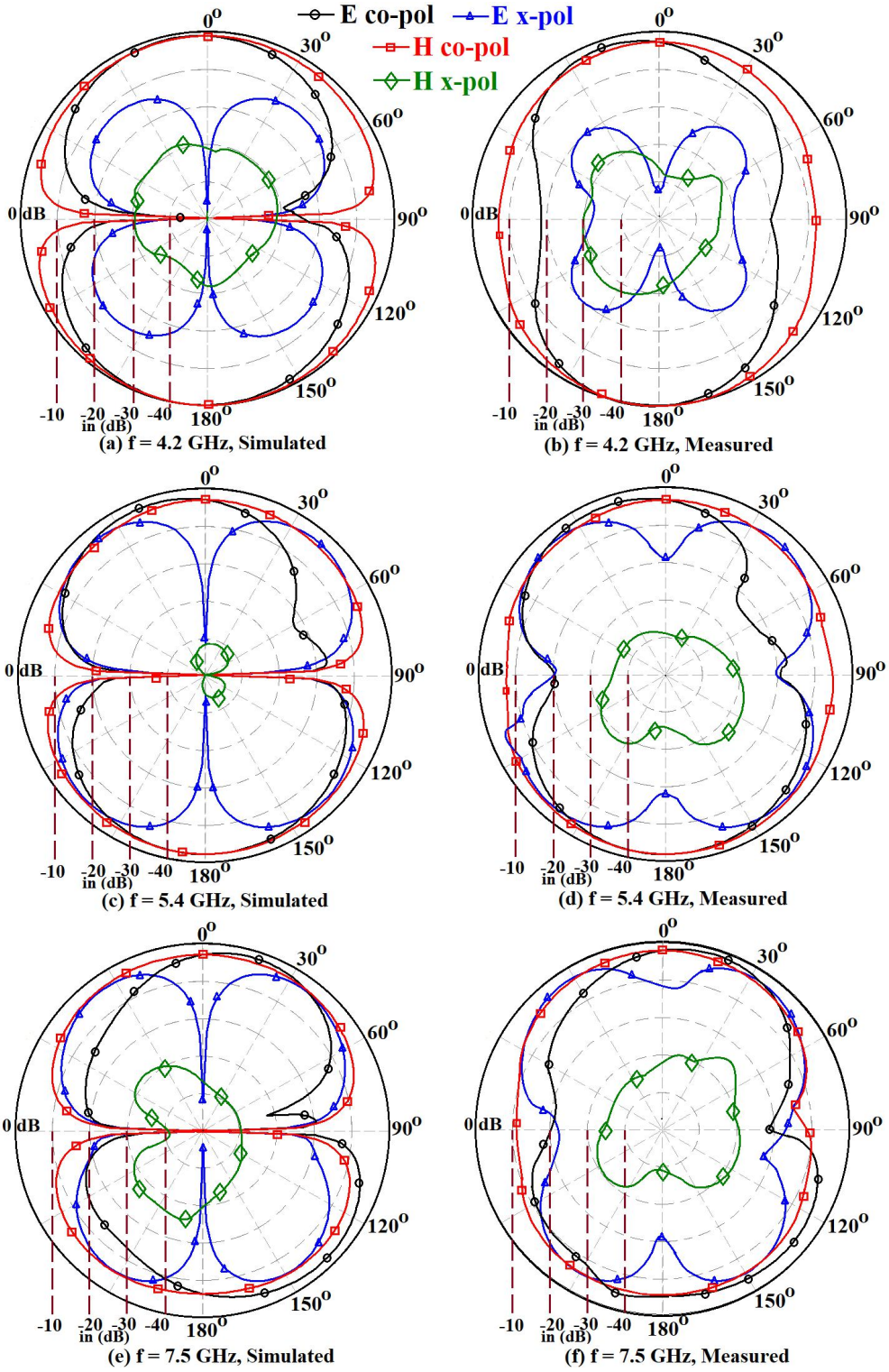

Fig. 11. Simulated and measured E-field (yz-plane) and H-field (xz-plane) radiation patterns in the pass bands.

The performance of the UWB antenna in the time domain is important in pulsed communication. The parameter group delay characterizes the time delay of an impulse signal at various frequencies. The time-domain parameters measurement has been done using Keysight Technologies make (N9917A) VNA in the free space environment wherein two alike band-notched antennas connected to two ports of VNA are spaced in face-to-face and side-by-side configurations at a distance of 300 mm

© 2021 SBMO/SBMag CC BY
ISSN 2179-1074

ensuring far-field distance. The simulated and measured S_{21} (transfer function) and group delay for both configurations are shown in *Fig.* 12(a) and (b), respectively. It is evident from *Fig.* 12(a, b) that the considerable delay in signal is observed at notched frequencies, whereas at other frequencies group delay for both configurations is almost constant. It is seen from, *Fig.* 12(a, b) that in both configurations S_{21} is less than 40 dB at notched frequencies. The time-domain analysis evidence that the proposed antenna is suitable for triple band-notched functions in the mentioned bands.

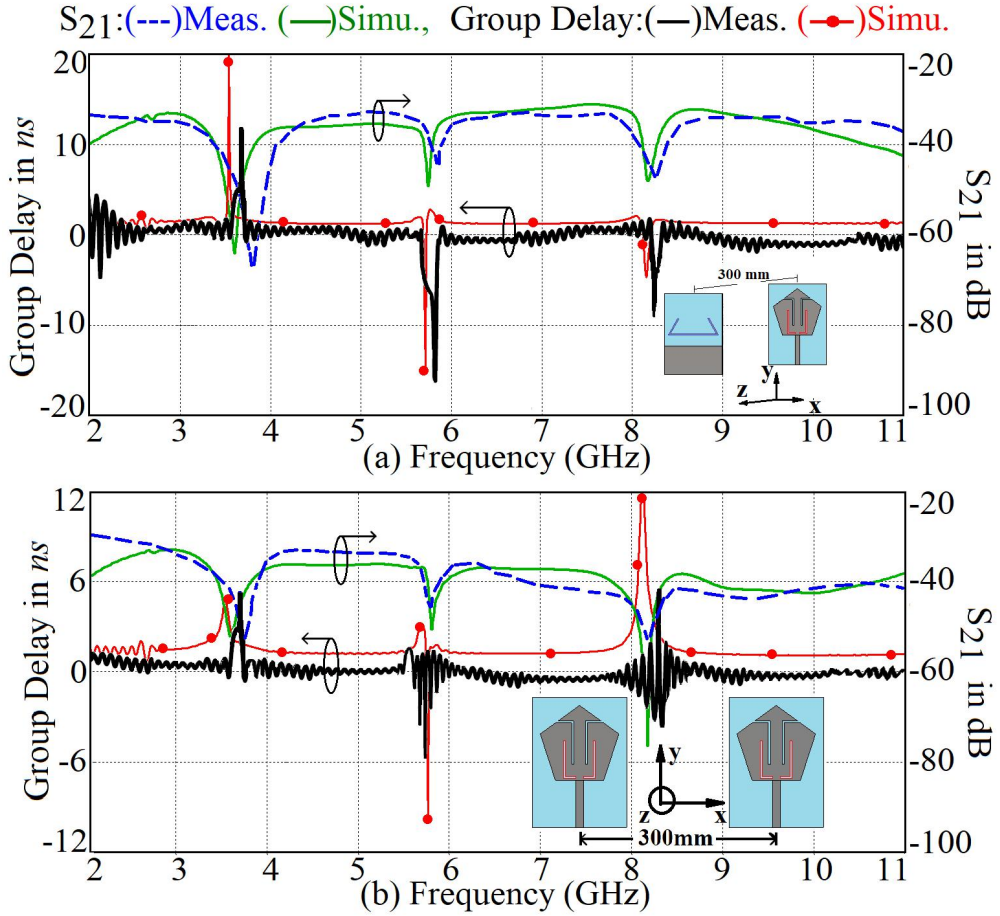

Fig. 12. Simulated and measured group delay and S_{21} of the proposed triple band-notch UWB antenna (a) face to face and (b) side by side configuration.

Comparison of antenna size and the number of notch bands of the proposed antenna with reported single, dual and triple band-notched UWB antennas are shown in Table 1. The notch band responses are obtained by placing two square EBG structures [16] and slitted EBGs near the feedline in [17]. Slots are incorporated in the patch to realize band notch responses, but the use of a dielectric resonator increases the volume of the antenna significantly [18], [25]. The combination of slots in the patch and SRR structures in the vicinity of the feedline is used to realize multiple band-notched responses [19]-[21]. The selection of placement of slots to obtain a notched band is not explained in terms of perturbation of modes [20]. The position of complementary SRR structures to realize notch bands is not explained in terms of modes or change in input impedance [21]. The band notch response is obtained by incorporating a ∩-slot in the feed line [22]. The rectangular strip is connected to the

© 2021 SBMO/SBMag CC BY
ISSN 2179-1074

radiator through vias to realize dual band-notch responses which increase fabrication complexity [23] To attain a single band-notched response in differential-fed antenna, two pairs of λ/4 length stubs are introduced in the ground plane [24]. The cylindrical dielectric resonator along with a U-shape slot is realised to obtain a single band notch response, but the use of a dielectric resonator increases the volume of the antenna.

TABLE I. COMPARISON WITH REPORTED SINGLE, DUAL AND TRIPLE BAND NOTCHED UWB ANTENNAS

Reference	Antenna size (mm^2)	Notched bands	Operating Frequency Range (GHz)
[16]	52 × 32 = 1664	2	3.11-10.60
[17]	30 × 40 = 1200	2	2.80-11.00
[18]	50 × 40 = 2000	2	2.90-10.82
[19]	78 × 45= 3478	2	2.63–10.86
[20]	38 × 34 = 1292	3	2.58-11.62
[21]	35 × 35 = 1225	3	2.31-12.83
[22]	34 × 34 = 1156	1	3.10–10.60
[23]	40 × 43 = 1720	2	2.90-11.00
[24]	35 × 30 = 1050	1	3.10-12.00
[25]	40 × 50 = 2000	1	3.30-12.00
This paper	32 × 24 = 768	3	2.71-11.00

In the reported literature mentioned in Table 1, the designed antennas have a larger dimension or have more complexity in terms of fabrication of structures. Also, the earlier reported works do not explain the modal analysis of the structure and perturbation of current at a particular mode to create impedance mismatch resulting in a notch response. The novelty of this work is the inclusion of detailed modal analysis to realize the notched characteristics in the proposed structure. Also, the proposed antenna has compact volume of 584 mm^3 and is capable of producing three notch bands.

V. CONCLUSIONS

A detailed study to explain the resonant mode behavior in printed pentagonal shape monopole antenna is presented. It shows that in printed monopole patch fundamental and second-order mode frequencies are the modified half-wavelength resonant modes. Further, a microstrip line fed pentagonal shape UWB antenna is proposed yielding impedance bandwidth in the range of 2.7 GHz to 10.6 GHz. UWB antenna design is further modified by incorporating a pair of mirrored Γ- and L-shape slots along with bent C-shape parasitic resonator to obtain tunable triple notch responses in WiMAX, WLAN, and ITU-T frequency band respectively. The Γ-shape and L-shape slots increase the impedance at TM_{21} and TM_{31} modes respectively realising band rejection across WiMAX and ITU-T frequency band. The bent C-shape resonator increases the input impedance at TM_{02} mode resulting in a notch function in the WLAN band. The surface current distributions at the realised notched frequency in the presence and absence of slots and parasitic resonators are also investigated. The proposed antenna exhibits an omnidirectional radiation pattern in H-plane while figure-of-eight

 © 2021 SBMO/SBMag CC BY *ISSN 2179-1074*

like patterns within the UWB spectrum except in the notched band. The proposed antenna also provides linear transfer function and negligible group delay variation excluding notched bands.

REFERENCES

[1] "Federal Communications Commission Revision of Part 15 of the Commission ' s Rules Regarding Ultra-Wideband Transmission System from 3.1 to 10.6 GHz," in FEDERAL Communications Commission. Washington, DC: ETDocket, pp. 98–153, FCC, 2002.
[2] K. P. Ray, "Design Aspects of Printed Monopole Antennas for Ultra-Wide Band Applications," *Int. J. Antennas Propag.*, vol. 2008, pp. 1–8, 2008.
[3] N. C. Azenui and H. Y. D. Yang, "A Printed crescent patch antenna for ultrawideband applications," *IEEE Antennas Wirel. Propag. Lett.*, vol. 6, pp. 113–116, 2007.
[4] K. P. Ray, S. S. Thakur, and R. A. Deshmukh, "UWB printed sectoral monopole antenna with dual polarization," *Microw. Opt. Technol. Lett.*, vol. 54, no. 9, pp. 2066–2070, 2012.
[5] C.-Y. Huang and W.-C. Hsia, "Planar elliptical antenna for ultra-wideband communications," *Electron. Lett.*, vol. 41, no. 6, pp. 40–41, 2005.
[6] K. J. Babu, B. K. Kumar, S. R. Boddu, and A. M. Varaprasad, "Design of a compact elliptical slot printed UWB antenna with band-notched characteristic," *Int. J. Electron. Lett.*, vol. 7, no. 4, pp. 448–457, 2019.
[7] P. S. Bakariya, S. Dwari, and M. Sarkar, "Triple band notch UWB printed monopole antenna with enhanced bandwidth," *AEU - Int. J. Electron. Commun.*, vol. 69, no. 1, pp. 26–30, 2015.
[8] A. A. Deshmukh and P. V. Mohadikar, "Modified rectangular shape patch antennas for ultra-wide band and notch characteristics response," *Microw. Opt. Technol. Lett.*, vol. 59, no. 7, pp. 1524–1529, 2017.
[9] B. Yang and S. Qu, "A compact integrated Bluetooth UWB dual-band notch antenna for automotive communications," *AEU - Int. J. Electron. Commun.*, vol. 80, pp. 104–113, 2017.
[10] O. M. H. Ahmed and A. R. Sebak, "Numerical and experimental investigation of a novel ultrawideband butterfly shaped printed monopole antenna with bandstop function," *Prog. Electromagn. Res. C*, vol. 18, pp. 111–121, 2011.
[11] A. M. Abbosh, "Design of a CPW-Fed Band-Notched UWB Antenna Using a Feeder-Embedded Slotline Resonator," *Int. J. Antennas Propag.*, vol. 2008, pp. 1–5, 2008.
[12] S. K. Mishra and J. Mukherjee, "Compact printed dual band-notched U-shape UWB antenna," *Prog. Electromagn. Res. C*, vol. 27, pp. 169–181, 2012.
[13] H. S. Mewara, J. K. Deegwal, and M. M. Sharma, "A slot resonators based quintuple band-notched Y-shaped planar monopole ultra-wideband antenna," *AEU - Int. J. Electron. Commun.*, vol. 83, pp. 470–478, 2018.
[14] M. Sharma, Y. K. Awasthi, and H. Singh, "CPW-fed triple high rejection notched UWB and X-band antenna on silicon for imaging and wireless applications," *Int. J. Electron.*, vol. 106, no. 7, pp. 945–959, 2019.
[15] N. Jaglan, B. K. Kanaujia, S. D. Gupta, and S. Srivastava, "Design of band-notched antenna with DG-CEBG," *Int. J. Electron.*, vol. 105, no. 1, pp. 58–72, 2018.
[16] T. Mandal and S. Das, "Design of dual notch band UWB printed monopole antenna using electromagnetic-bandgap structure," *Microw. Opt. Technol. Lett.*, vol. 56, no. 9, pp. 2195–2199, 2014.
[17] M. Ghahremani, C. Ghobadi, J. Nourinia, M. S. Ellis, F. Alizadeh, and B. Mohammadi, "Miniaturised UWB antenna with dual-band rejection of WLAN/WiMAX using slitted EBG structure," *IET Microwaves, Antennas Propag.*, 2019.
[18] T. A. Denidni and Z. Weng, "Hybrid ultrawideband dielectric resonator antenna and band-notched designs," *IET Microwaves, Antennas Propag.*, vol. 5, no. 4, pp. 450–458, 2011.
[19] L. C. Tsai, "A ultrawideband antenna with dual-band band-notch filters," *Microw. Opt. Technol. Lett.*, vol. 59, no. 8, pp. 1861–1866, 2017.
[20] S. Kundu and S. K. Jana, "Leaf-shaped CPW-fed UWB antenna with triple notch bands for ground penetrating radar applications," *Microw. Opt. Technol. Lett.*, vol. 60, no. 4, pp. 930–936, 2018.
[21] D. Sarkar, K. V. Srivastava, and K. Saurav, "A compact microstrip-fed triple band-notched UWB monopole antenna," *IEEE Antennas Wirel. Propag. Lett.*, vol. 13, pp. 396–399, 2014.
[22] Y. K. Choukiker and S. K. Behera, "Modified Sierpinski square fractal antenna covering ultra-wide band application with band notch characteristics," *IET Microwaves, Antennas Propag.*, vol. 8, no. 7, pp. 506–512, 2014.
[23] F. Zhu *et al.*, "Dual band-notched tapered slot antenna using λ/4 band-stop filters," *IET Microwaves, Antennas Propag.*, vol. 6, no. 15, pp. 1665–1673, 2012.
[24] J. Zhang, T. Chen, L. Hua, and W. Wang, "A compact differential-fed UWB antenna with band-notched characteristics," *Prog. Electromagn. Res. M*, vol. 83, no. 8 pp. 171–179, 2019.
[25] M. Debab and Z. Mahdjoub, "Single band notched characteristics UWB antenna using a cylindrical dielectric resonator and U-shaped slot," *J. Microwaves, Optoelectron. Electromagn. Appl.*, vol. 17, no. 3, pp. 340–351, 2018.
[26] A. A. Kadam and A. A. Deshmukh, "Pentagonal Shaped UWB Antenna Loaded with Slot and EBG Structure for Dual Band Notched Response," *Progress In Electromagnetics Research M*, Vol. 95, pp. 165-176, 2020.
[27] E. O. Hammerstad, "Equations for microstrip circuit design," *Proceedings of the European Microwave Conference,* Hamburg, Germany, 1975, pp. 268–272.

received 13 Dec 2020; for review 28 Dec 2020; accepted 8 Apr 2021
© 2021 SBMO/SBMag CC BY
ISSN 2179-1074